



**HAL**  
open science

# Monitoring squeezed collective modes of a 1D Bose gas after an interaction quench using density ripples analysis

Max Schemmer, Aisling Johnson, Isabelle Bouchoule

## ► To cite this version:

Max Schemmer, Aisling Johnson, Isabelle Bouchoule. Monitoring squeezed collective modes of a 1D Bose gas after an interaction quench using density ripples analysis. 2017. hal-01661074v6

**HAL Id: hal-01661074**

**<https://iogs.hal.science/hal-01661074v6>**

Preprint submitted on 16 May 2018 (v6), last revised 15 Nov 2018 (v8)

**HAL** is a multi-disciplinary open access archive for the deposit and dissemination of scientific research documents, whether they are published or not. The documents may come from teaching and research institutions in France or abroad, or from public or private research centers.

L'archive ouverte pluridisciplinaire **HAL**, est destinée au dépôt et à la diffusion de documents scientifiques de niveau recherche, publiés ou non, émanant des établissements d'enseignement et de recherche français ou étrangers, des laboratoires publics ou privés.

# Monitoring squeezed collective modes of a 1D Bose gas after an interaction quench using density ripples analysis

Max Schemmer, Aisling Johnson,\* and Isabelle Bouchoule<sup>†</sup>  
*Laboratoire Charles Fabry, Institut d'Optique, CNRS, Universit Paris Sud 11,  
 2 Avenue Augustin Fresnel, F-91127 Palaiseau Cedex, France*

(  
 (Dated: May 16, 2018)

We investigate the out-of-equilibrium dynamics following a sudden quench of the interaction strength, in a one-dimensional quasi-condensate trapped at the surface of an atom chip. Within a linearized approximation, the system is described by independent collective modes and the quench squeezes the phase space distribution of each mode, leading to a subsequent breathing of each quadrature. We show that the collective modes are resolved by the power spectrum of density ripples which appear after a short time of flight. This allows us to experimentally probe the expected breathing phenomenon. Our results are in good agreement with theoretical predictions which take the longitudinal harmonic confinement into account.

The out-of-equilibrium dynamics of isolated quantum many-body systems is a field attracting a lot of interest. On the theoretical side, many questions are currently investigated and debated. Whether and how the system relaxes towards an equilibrium state is in particular the subject of intense work and the role of integrability is still not completely clear. A particular focus has been devoted to the case of sudden quenches where the system is brought out-of-equilibrium by a sudden change of a Hamiltonian parameter [1, 2][3], and in particular the case of an interaction quench. On the experimental side, the subsequent evolution of correlation functions has been investigated in several experiments [4, 5]. In particular in [5], a light cone effect has been observed in the first order correlation function after splitting a 1D Bose gas into two copies. After the light-cone extends over a few correlation lengths the system showed thermalization [6]. However, this apparent thermalization may conceal an underlying non-equilibrium behavior. This is especially true for integrable or quasi-integrable systems where the system might not relax towards a Gibbs ensemble. In a recent experiment, long term non-equilibrium dynamics has been revealed by a revival phenomenon [7], although the dynamics at play before the revival were not visible in the first order correlation function. Finding proper observables revealing the dynamics is thus a key point for investigating out-of-equilibrium phenomena.

In this paper, we investigate the out-equilibrium dynamics following a sudden quench of the interaction strength in a quasi-1D Bose gas with repulsive interactions. While the complete treatment is tremendously difficult and has been the subject of several theoretical studies [8–10], the problem is greatly simplified if one can rely on a linearized approach. For each collective mode one then expects the quench to produce a squeezed phase space distribution, leading to a subsequent oscillation of each quadrature width — a *breathing behavior*. These oscillatory dynamics are *a priori* not visible if one considers observables mixing different modes, such as the

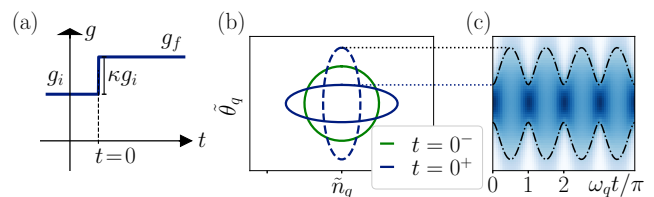


FIG. 1. Squeezing of each collective mode after an interaction strength quench. The Gaussian space distributions before the quench (green circle), just after the quench (solid ellipse) and after an evolution time  $\pi/(2\omega_q)$  (dashed ellipse) are represented in (b), where lines correspond to a given probability density. The subsequent breathing is seen in (c), where the time evolution of the phase distribution is shown.

one-body correlation function. The dephasing between modes then leads to an apparent thermalization, occurring on a relatively short time. We show in this paper that individual collective modes may be monitored using an analysis of the density ripples appearing after short time of flight. Experimentally, we observe the breathing of squeezed modes, revealing the mechanism at play after an interaction quench. In the first part of the paper, we present the theoretical framework predicting the expected squeezing and subsequent dynamics of each collective mode. We then expose why density ripples give access to the dynamics of individual modes. Finally, we present our experimental results and compare them to the derived theoretical predictions.

The relevant physics can be understood by considering a 1D homogeneous Bose gas, of length  $L$  and density  $n_0$ , with particles of mass  $m$  interacting with repulsive contact interactions  $g\delta(z_i - z_j)$  at a temperature  $T$ . At  $t = 0$ ,  $g$  is suddenly changed from  $g_i$  to  $g_f = (1 + \kappa)g_i$ , where  $\kappa$  is the quench strength. Within the quasi-condensate regime, density fluctuations are strongly reduced ( $|\delta n(z)| \ll n_0$ ) and phase fluctuations occur on large length scales, such that the

Hamiltonian of the system can be diagonalized using the phase-density representation of the field operator  $\Psi(z) = \sqrt{n_0 + \delta n(z)} \exp(i\theta(z))$  and the Bogoliubov procedure [11]. The obtained linearized modes correspond to Fourier modes. For each wave-vector  $q$ , the dynamics is governed by the harmonic oscillator Hamiltonian [12]

$$H_q = A_q n_q^2 + B_q \theta_q^2 = \hbar\omega_q \left( \frac{\tilde{n}_q^2}{2} + \frac{\tilde{\theta}_q^2}{2} \right) \quad (1)$$

where the canonically conjugated hermitian operators  $n_q$  and  $\theta_q$  are the Fourier components [13] of  $\delta n$  and  $\theta$  and where the reduced variables are defined by  $\tilde{n}_q = n_q(A_q/B_q)^{1/4}$  and  $\tilde{\theta}_q = \theta_q(B_q/A_q)^{1/4}$ . For wavevectors  $q$  much smaller than the inverse healing length  $\xi^{-1} = \sqrt{mgn_0}/\hbar$ , the excitations are of hydrodynamic nature [14]. Their frequency is  $\omega_q = cq$ , where the speed of sound is  $c = \sqrt{n_0 \partial_n \mu / m}$ , and the Hamiltonian's coefficients are  $B_q = \hbar^2 q^2 n_0 / (2m)$  and  $A_q = c^2 / (2n_0)$ . Here  $\mu(n)$  is the equation of state of the gas relating the chemical potential  $\mu$  to the linear density, which reduces to  $\mu = gn$  for pure 1D quasi-condensate. For a given  $q$ , the dynamics of the quenched harmonic oscillator is represented Fig. (1). Before the quench the phase space distribution is the one of a thermal state: an isotropic Gaussian in the  $(\tilde{\theta}_q, \tilde{n}_q)$ -plane. The quench affects  $A_q$  while  $\theta_q$  and  $n_q$  do not have time to change. The variances thus become  $\langle \tilde{\theta}_q^2 \rangle_{t=0+} = \langle \tilde{\theta}_q^2 \rangle_{t=0-} / (1 + \kappa)^{1/4}$  and  $\langle \tilde{n}_q^2 \rangle_{t=0+} = (1 + \kappa)^{1/4} \langle \tilde{n}_q^2 \rangle_{t=0-}$  [15]. The subsequent evolution is a rotation in phase space at a frequency  $\omega_q$  leading to a breathing of each quadrature. In particular

$$\langle \theta_q^2 \rangle = \langle \theta_q^2 \rangle_i (1 + \kappa \sin^2(cqt)), \quad (2)$$

where the initial value  $\langle \theta_q^2 \rangle_i$  is the thermal prediction  $\langle \theta_q^2 \rangle = mk_B T / (\hbar^2 n_0 q^2)$  [16].

Probing the non equilibrium dynamics following a quench is not straightforward, especially concerning the choice of observable. Since density fluctuations are very small within the quasi-condensate regime, it is more advantageous to probe the phase fluctuations. For this purpose, one way is to investigate the one-body correlation function  $g_1(z) = \langle \hat{\Psi}(z)^\dagger \hat{\Psi}(0) \rangle$ , which can for instance be measured via its Fourier transform, the momentum distribution [17]. For distances much larger than  $\xi$ , density fluctuations give a negligible contribution and, for Gaussian distributions of  $\theta$ , the Wick theorem gives  $g_1(z) \simeq n_0 e^{-((\theta(z) - \theta(0))^2)/2}$ . However since phase fluctuations are large in a quasi-condensate, the exponential cannot be linearized and  $g_1(z)$  mixes contributions from all Bogoliubov modes [18], preventing the observation of the squeezed dynamics. In fact, the linearized model above predicts the light-cone effect on the  $g_1$  function:  $g_1(z)$  changes from its initial exponential decay  $\exp(-|z|/l_c^i)$ , where  $l_c^i = 2\hbar^2 n_0 / (mk_B T)$ , to an exponential decay with a new correlation length  $l_c^f = 2l_c^i / (\kappa + 2)$

for  $z < 2ct$ . The breathing of each squeezed Bogoliubov mode is not transparent here. Moreover, for times larger than a few  $t_{\text{th}}^i = l_c^i / c$ , the  $g_1$  function essentially reaches the form expected for a thermal state at a temperature  $T_f = T(\kappa + 2)/2$ , and the ongoing dynamics is hidden. In this paper we use the density ripples analysis to reveal the non equilibrium dynamics of the gas by probing the breathing of each mode.

Density ripples appear after switching the interactions off and waiting for a free evolution time  $t_f$  (time-of-flight), during which phase fluctuations transform into density fluctuations [19]. The analysis of these density ripples has been used as thermometry [20, 21], and to investigate the cooling mechanism [22]. Consider the power spectrum of density ripples  $\langle |\rho(q)|^2 \rangle$ , where  $\rho(q) = (1/\sqrt{L}) \int dz (\langle n(z, t_f) \rangle - n_0) e^{iqz}$ . Propagating the field operator during the time of flight and assuming translational invariance we obtain [23]

$$\langle |\rho_{n_0}(q)|^2 \rangle = \int dx e^{-iqx} (f(q, x) - n_0^2), \quad (3)$$

where

$$\begin{aligned} f(q, x) &= \langle \psi^+(0) \psi(-\hbar q t_f / m) \psi^+(x - \hbar q t_f / m) \psi(x) \rangle \\ &\simeq n_0^2 \langle e^{i[\theta(0) - \theta(-\hbar q t_f / m) + \theta(x - \hbar q t_f / m) - \theta(x)]} \rangle, \end{aligned} \quad (4)$$

averages in Eq. (4) being taken before the time of flight. The function  $f$  involves only pairs of points separated by  $\hbar q t_f / m$ . For small wave vectors  $q \hbar t_f / m \ll l_c$ , the phase difference between those points is small and one can expand the exponential. To lowest order, assuming uncorrelated distributions for each mode  $q$  and vanishing mean values, we then find

$$\langle |\rho_{n_0}(q)|^2 \rangle = 4n_0^2 \langle \theta_q^2 \rangle \sin^2 \left( \frac{\hbar q^2 t_f}{2m} \right), \quad (5)$$

showing that, for low lying  $q$ , the density ripples spectrum directly resolves the phase quadrature  $\langle \theta_q^2 \rangle$  of individual Bogoliubov modes [24]. The proportionality between  $\langle |\rho_{n_0}(q)|^2 \rangle$  and  $\langle \theta_q^2 \rangle$  implies that  $\langle |\rho_{n_0}(q)|^2 \rangle$  oscillates according to Eq. (2) when varying the time  $t$  after the quench. Density ripples are thus an ideal tool to investigate the quench dynamics.

In typical experiments, atoms are confined by a smooth potential  $V(z)$ , generally harmonic, which complicates the picture. However, if the confinement is weak enough and for wavelengths much smaller than the system's size, one can use the above results for homogeneous systems within a local density approximation (LDA). More precisely,  $\tilde{\rho}(q) = \int dz \delta n(z, t_f) e^{iqz}$  fulfills  $\langle |\tilde{\rho}(q)|^2 \rangle = \int dz \langle |\rho_{n_0(z)}(q)|^2 \rangle$  where  $n_0(z)$  is the density profile. The latter can itself be evaluated within the LDA using the gas equation of state and the local chemical potential  $\mu(z) = \mu_0 - V(z)$ . Injecting Eq. (2) and Eq. (5) into the LDA integral above, we find

$$\langle |\tilde{\rho}(q)|^2 \rangle / \langle |\tilde{\rho}(q)|^2 \rangle_i = 1 + \kappa \mathcal{F}(cqt), \quad (6)$$

where  $c$  is the speed of sound after the quench evaluated at the trap center and  $\mathcal{F}$  only depends on the shape of  $V(z)$ . The explicit expression of  $\mathcal{F}$  in the case of a harmonic potential is given in [25]. Since the central part of the cloud gives the dominant contribution,  $\langle |\tilde{\rho}(q)|^2 \rangle$  still presents an oscillatory behavior as a function of  $t$ ,  $\mathcal{F}(\tau)$  being close to  $\sin^2(\tau)$ . The spread in frequencies originating from the inhomogeneity in  $n_0$  is however responsible for a damping, which is a pure dephasing effect.

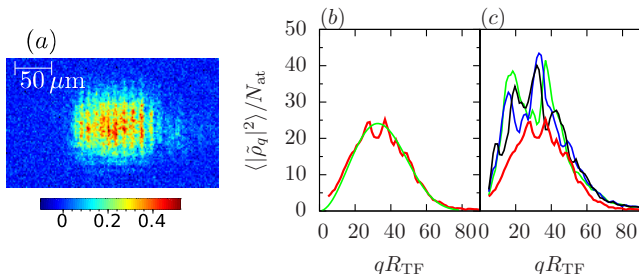


FIG. 2. Density ripples analysis. (a) Typical absorption image (optical density shown) taken after a time-of-flight  $t_f = 8$  ms. (b) Power spectrum of density ripples, obtained by averaging over about 50 images, for a cloud at thermal equilibrium containing 16000 atoms confined in a trap with frequencies  $\omega_z/(2\pi) = 8.5$  Hz and  $\omega_\perp/(2\pi) = 1.5$  kHz, yielding a Thomas-Fermi radius  $R_{TF} = 75 \mu\text{m}$ . The green line is a theoretical fit (see text), yielding a temperature  $T = 55$  nK and an optical resolution  $\sigma = 2.9 \mu\text{m}$ . (c) Power spectra after a quench of strength  $\kappa = 2$ , at times  $t = 2.1$ ms (green),  $t = 2.6$ ms (blue) and  $t = 4.6$ ms (black), the thick red curve being the initial power spectrum.

The experiment uses an atom-chip set up [26] where atoms are magnetically confined using current-carrying micro-wires. The transverse confinement is provided by three parallel wires carrying AC-current modulated at 400 kHz, which renders the magnetic potential insensitive to wire imperfections and, allows for independent control of the transverse and longitudinal confinements. We perform radio frequency (RF) forced evaporative cooling until we reach the desired temperature. We then increase the RF frequency by 60 kHz, providing a shield for energetic three-body collision residues and wait during 150 ms relaxation time [27]. The clouds contain a few thousand atoms, in a trap with a transverse frequency  $\omega_\perp/2\pi = 1.5 - 3.1$  kHz and a longitudinal frequency  $\omega_\parallel/2\pi = 8.5$  Hz. The samples are quasi-1D, the temperature and chemical potential satisfying  $\mu, k_B T < \hbar\omega_\perp$ . The temperature is low enough so that the gas typically lies well within the quasi-condensate regime [28]. The equation of state is well described by  $\mu = \hbar\omega_\perp(\sqrt{1 + 4na} - 1)$ , where  $a = 5.3$  nm is the 3D scattering length [29]. While, for  $na \ll 1$ , one recovers the pure 1D expression  $\mu = gn$ , where  $g = 2\hbar\omega_\perp a$ , this equation of state takes the broadening of the transverse size at larger  $na$  into account. The longitudinal density profile, well described

by the LDA, extends over twice the Thomas-Fermi radius  $R_{TF} = \sqrt{2\mu_0/m}/\omega_z$ . The speed of sound derived from the equation of state is  $c = c_{1D}/(1 + 4na)^{1/4}$  where  $c_{1D} = \sqrt{2\hbar\omega_\perp na/m}$  is the pure 1D expression. For data presented in this paper,  $c/c_{1D}$  is close to 0.7. Since the effective interaction strength is proportional to  $c^2$ , it is proportional to  $\omega_\perp$ .

The interaction strength quench therefore amounts to ramping the transverse trapping frequency  $\omega_\perp$  from its initial value  $\omega_{\perp,i}$  to its final value  $\omega_{\perp,f} = (1 + \kappa)\omega_{\perp,i}$  within a time  $t_r$ , typically of the order of 1 ms. This time is long enough for the transverse motion of the atoms to follow adiabatically but short enough so that the quench can be considered as almost instantaneous with respect to the probed longitudinal excitations [25]. In order to avoid dynamics of the mean profile and modification of the Bogoliubov wavefunctions [25], we simultaneously adapt the longitudinal trapping frequency, such that the Thomas-Fermi radius stays constant.

In order to probe density ripples, we release the atoms from the trap and let them fall under gravity for a time  $t_f = 8$  ms before taking an absorption image. The transverse expansion, occurring on a time scale of  $1/\omega_\perp$ , ensures the effective instantaneous switching off of the interactions with respect to the probed longitudinal excitations. The density ripples produced by the phase fluctuations present before the free fall are visible in each individual image, as seen in Fig. (2)(a). From the image, we record the longitudinal density profile  $\rho(z, t_f)$  and its discrete Fourier transform [30]  $\tilde{\rho}(q)$ . We acquire about 40 images taken in the same conditions with atom number fluctuations smaller than 10%. From this data set, we then extract the power spectrum  $\langle |\tilde{\rho}(q)|^2 \rangle$ . We note  $\langle |\tilde{\rho}(q)|^2 \rangle_i$  the power spectrum obtained before the quench and a typical spectrum is shown in Fig. (2)(b). We chose to normalize the momenta by  $R_{TF}^{-1}$ : since the Fourier distribution of the  $i^{\text{th}}$  Bogoliubov mode of a 1D quasi-condensate is peaked at  $k_i \simeq i/R_{TF}$  [25], the x-axis roughly corresponds to the mode index. The predicted power spectrum  $\langle |\tilde{\rho}(q)|^2 \rangle_{\text{th}}$  is computed using the LDA and analytical solution of Eq. (3) for thermal equilibrium [25][31]. This expression is peaked around  $kR_{TF} \simeq \sqrt{\pi m/(\hbar t_f)} R_{TF} \simeq 50$ . For comparison with experimental data, we take the imaging resolution into account by multiplying  $\langle |\tilde{\rho}(q)|^2 \rangle_{\text{th}}$  with  $e^{-k^2\sigma^2/2}$  where  $\sigma$  is the rms width of the impulse imaging response function, assumed to be Gaussian. The experimental data ultimately compared well with the theoretical predictions, as shown in Fig. (2)(b), where  $T$  and  $\sigma$  are obtained by fitting the data [32].

We then investigate the dynamics following the quench of the interaction strength by acquiring power spectra of density ripples at different evolution times  $t$  after the quench. We typically acquire power spectra every 0.5 ms, over a total time of 5 ms. A few raw spectra are shown in Fig. (2)(c), for a quench strength  $\kappa = 2.0$ . At first sight

the power spectra seem erratic. In order to reveal the expected oscillatory behavior of each Fourier component we introduce, for each wavevector  $q$  of the discrete Fourier transform, and each measurement time  $t$ , the reduced time  $\tau = cqt$ , where  $c$  is evaluated for the central density, and compute  $J(q, \tau) = \langle |\tilde{\rho}(q)|^2 \rangle(t) / \langle |\tilde{\rho}(q)|^2 \rangle_i$ . We restrict the range of  $q$  values to  $10 < qR_{TF} < 40$ , to ensure both the condition  $q\hbar t_v/m \ll l_c$  and the validity of the LDA. On the resulting set of sparse data, shown in the inset of Fig. (3), an oscillatory behavior appears, despite noise on the data. To combine all the data in a single graph, we perform a “smooth” binning in  $\tau$ , *i.e.* we compute, for any given reduced time  $\tau$ , the weighted averaged of the data with a Gaussian weight function in  $\tau$  of width  $\Delta = 0.31$ : namely we compute  $\bar{J}(\tau) = \sum_{\alpha} J(q_{\alpha}, \tau_{\alpha}) e^{-(\tau_{\alpha} - \tau)^2 / (2\Delta^2)} / \sum_{\alpha} e^{-(\tau_{\alpha} - \tau)^2 / (2\Delta^2)}$ , where the sum is done on the data set. The function  $\bar{J}(\tau)$ , shown in Fig. (3) shows a clear oscillatory behavior.

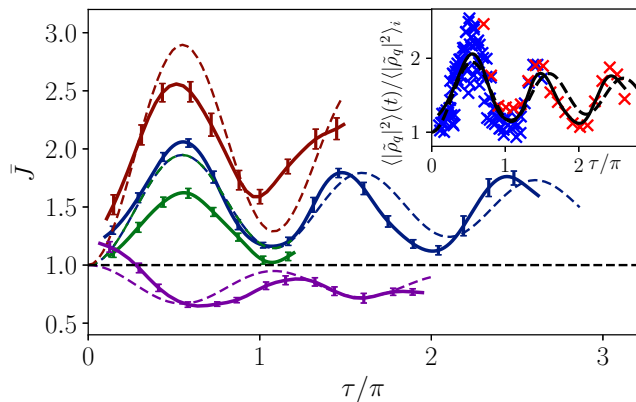


FIG. 3. Time evolution of squeezed collective modes produced by an interaction strength. The normalized density ripples power spectrum is plotted versus the reduced time  $\tau = cqt$ , where the speed of sound  $c$  is calculated for the central density. Inset shows the data corresponding to each measurement time and discrete  $q$  values, for a data set corresponding to  $\kappa = 2$  and  $\omega_{\perp, i} = 2\pi \times 1.5$  kHz, together with the resulting averaged quantity  $\bar{J}$  (see text) and the theoretical prediction for  $\kappa = 1$  (dashed). Points in blue correspond to  $t < t_{\text{th}}^{g_1}$  and red to  $t > t_{\text{th}}^{g_1}$ . The main graph shows the evolution of  $\bar{J}$  for different data sets. The initial transverse oscillation frequency is 1.5 kHz, except for the green curve for which it is 3 kHz. Quench strengths are  $\kappa = 4$  (red data),  $\kappa = 2$  (blue and green) data and  $\kappa = -0.7$  (purple data). Dashed lines are theoretical predictions for quench strengths  $\kappa = 2$  (red), 1 (blue/red) and  $-0.35$  (purple).

We repeat the experiment for different quench strengths  $\kappa = (\omega_{\perp, f} / \omega_{\perp, i} - 1) = \{0.3, 3, 5\}$ , and initial trapping oscillation frequencies  $\omega_{\perp} = \{3, 1.5\}$  kHz. The oscillatory behavior is present in all cases as shown in Fig. (3). We compared the observed oscillations with the theoretical predictions from the linearized model, Eq. (6).

The temporal behavior of the data is in good agreement with the predicted one: both the frequency and the observed damping are in agreement with the predictions. The amplitude of the experimental oscillations on the other hand are significantly smaller than the predictions, and in Fig. (3) we plot the theoretical predictions for quench strengths twice as small as the experimental ones. Moreover, for a given quench strength, the observed amplitude depend on the initial transverse frequency, in contradiction with the theoretical model. Several effects leading to a decrease of the oscillation amplitude are discussed in the [25]. However, they only partially account for the observed amplitude reduction.

In conclusion, analyzing density ripples, we revealed the physics at play after a sudden quench of the interaction strength in a quasi-1D Bose gas, namely the breathing associated to the squeezing of each collective mode. The observed out-of-equilibrium dynamics continues for times larger than  $t_{\text{th}}^{g_1}$ , for which the  $g_1$  function essentially reached its asymptotic thermal behavior [33] This can be seen in the inset of Fig. (3) where data corresponding to  $t > t_{\text{th}}^{g_1}$ , shown in red, still present an oscillatory behavior. This clearly underlines the power of density ripple analysis to unveil out-of-equilibrium physics. The observed damping is compatible with the sole dephasing effect due to the longitudinal harmonic confinement. At later times, the discreteness of the spectrum and its almost constant level spacing is expected to produce a revival phenomenon. Its observation might however be hindered by a damping of each collective mode due to non-linear couplings. Such a damping occurs, despite the integrability of the 1D Bose gas with contact repulsive interactions, because the Bogoliubov collective modes do not correspond to the conserved quantities. A long-lived non-thermal nature of the state produced by the interaction strength might be revealed either by observing excitations in both the phononic regime and the particle regime of the Bogoliubov spectrum [34], or, ideally, in finding a way to access the distribution of the Bethe-Ansatz rapidities.

This work was supported by Région Île de France (DIM NanoK, Atocirc project). The authors thank Dr Sophie Bouchoule of C2N (centre nanosciences et nanotechnologies, CNRS / UPSUD, Marcoussis, France) for the development and microfabrication of the atom chip. Alan Durnez and Abdelmounaim Harouri of C2N are acknowledged for their technical support. C2N laboratory is a member of RENATECH, the French national network of large facilities for micronanotechnology. M. Schemmer acknowledges support by the Studienstiftung des Deutschen Volkes.

- 
- \* current address Vienna Center for Quantum Science and Technology, TU Wien-Atominstytut, Stadionallee 2, 1020 Vienna, Austria.
- † isabelle.bouchoule@institutoptique.fr
- [1] S. Trotzky, Y.-A. Chen, A. Flesch, I. P. McCulloch, U. Schollwck, J. Eisert, and I. Bloch. Probing the relaxation towards equilibrium in an isolated strongly correlated one-dimensional Bose gas. *Nature Physics*, 8(4):nphys2232, February 2012.
- [2] Tim Langen, Thomas Schweigler, Eugene Demler, and Jrg Schmiedmayer. Double light-cone dynamics establish thermal states in integrable 1d Bose gases. *arXiv:1709.05994 [cond-mat, physics:quant-ph]*, September 2017. arXiv: 1709.05994.
- [3] See [35] and references therein.
- [4] Marc Cheneau, Peter Barmettler, Dario Poletti, Manuel Endres, Peter Schau, Takeshi Fukuhara, Christian Gross, Immanuel Bloch, Corinna Kollath, and Stefan Kuhr. Light-cone-like spreading of correlations in a quantum many-body system. *Nature*, 481(7382):484–487, January 2012.
- [5] T. Langen, R. Geiger, M. Kuhnert, B. Rauer, and J. Schmiedmayer. Local emergence of thermal correlations in an isolated quantum many-body system. *Nat Phys*, 9(10):640–643, October 2013.
- [6] The degrees of freedom corresponding to antisymmetric variables showed thermalization, while the symmetric degrees of freedom were at another temperature. The system was thus pre-thermalized, and true thermalization between symmetric and antisymmetric degrees of freedom occurs at longer times.
- [7] Bernhard Rauer, Sebastian Erne, Thomas Schweigler, Federica Cataldini, Mohammadamin Tajik, and Jrg Schmiedmayer. Recurrences in an isolated quantum many-body system. *arXiv:1705.08231 [cond-mat, physics:quant-ph]*, May 2017. arXiv: 1705.08231.
- [8] Jacopo De Nardis, Bram Wouters, Michael Brockmann, and Jean-Sbastien Caux. Solution for an interaction quench in the Lieb-Liniger Bose gas. *Phys. Rev. A*, 89(3):033601, March 2014.
- [9] Pasquale Calabrese and Pierre Le Doussal. Interaction quench in a LiebLiniger model and the KPZ equation with flat initial conditions. *J. Stat. Mech.*, 2014(5):P05004, 2014.
- [10] M. A. Cazalilla and Ming-Chiang Chung. Quantum quenches in the Luttinger model and its close relatives. *J. Stat. Mech.*, 2016(6):064004, 2016.
- [11] Christophe Mora and Yvan Castin. Extension of Bogoliubov theory to quasicondensates. *Phys. Rev. A*, 67(5):053615, May 2003.
- [12] M. Schemmer, A. Johnson, R. Photopoulos, and I. Bouchoule. Monte Carlo wave-function description of losses in a one-dimensional Bose gas and cooling to the ground state by quantum feedback. *Phys. Rev. A*, 95(4):043641, April 2017.
- [13] For each positive  $q$  value, one has 2 Fourier components:  $\hat{n}_{q,c} = \sqrt{2/L} \int dz n(z) \cos(qz)$  and  $\hat{n}_{q,s} = \sqrt{2/L} \int dz n(z) \sin(qz)$ , with similar expressions for  $\theta$ . We omit the subscript  $c$  or  $s$  in the text for simplicity.
- [14] For quasi-1D gases the hydrodynamic condition is replaced by  $\omega_q \ll \omega_\perp$ .
- [15] The phase space area is preserved, one quadrature being squeezed, while the other is anti-squeezed.
- [16] For the  $q$  values considered,  $\omega_q \ll k_B T$  and the Raighley-Jeans approximation holds.
- [17] Thibaut Jacqmin, Bess Fang, Tarik Berrada, Tommaso Roscilde, and Isabelle Bouchoule. Momentum distribution of one-dimensional Bose gases at the quasicondensation crossover: Theoretical and experimental investigation. *Phys. Rev. A*, 86(4):043626, October 2012.
- [18] Isolating the contribution of individual modes to the function  $g_1(z)$  requires looking at the Fourier transform of  $\ln(g_1(z))$ , which requires large detection dynamics.
- [19] A. Imambekov, I. E. Mazets, D. S. Petrov, V. Gritsev, S. Manz, S. Hofferberth, T. Schumm, E. Demler, and J. Schmiedmayer. Density ripples in expanding low-dimensional gases as a probe of correlations. *Phys. Rev. A*, 80(3):033604, September 2009.
- [20] S. Dettmer, D. Hellweg, P. Ryytty, J. J. Arlt, W. Ertmer, K. Sengstock, D. S. Petrov, G. V. Shlyapnikov, H. Kreutzmann, L. Santos, and M. Lewenstein. Observation of Phase Fluctuations in Elongated Bose-Einstein Condensates. *Phys. Rev. Lett.*, 87(16):160406, October 2001.
- [21] S. Manz, R. Bcker, T. Betz, Ch. Koller, S. Hofferberth, I. E. Mazets, A. Imambekov, E. Demler, A. Perrin, J. Schmiedmayer, and T. Schumm. Two-point density correlations of quasicondensates in free expansion. *Phys. Rev. A*, 81(3):031610, March 2010.
- [22] B. Rauer, P. Griins, I.E. Mazets, T. Schweigler, W. Rohringer, R. Geiger, T. Langen, and J. Schmiedmayer. Cooling of a One-Dimensional Bose Gas. *Phys. Rev. Lett.*, 116(3):030402, January 2016.
- [23] For consistency we rederive this expression (first established in [19]) in [25].
- [24] In Eq. (5),  $\langle \theta_q^2 \rangle = (\langle \theta_{q,c}^2 \rangle + \langle \theta_{q,s}^2 \rangle)/2$  where  $\theta_{q,c}$  and  $\theta_{q,s}$  are the cosine and sine Fourier components, which fulfill  $\langle \theta_{q,c}^2 \rangle = \langle \theta_{q,s}^2 \rangle$  for translationally invariant systems.
- [25] See Supplementary Material. Supplementary material.
- [26] The experiment is described in more detail in [17].
- [27] We are aware that this initial state does not necessarily represent a thermal state []. However, the density ripples analysis only probes phonons, and their distribution is consistent with thermal equilibrium.
- [28] K. V. Kheruntsyan, D. M. Gangardt, P. D. Drummond, and G. V. Shlyapnikov. Pair Correlations in a Finite-Temperature 1d Bose Gas. *Phys. Rev. Lett.*, 91(4):040403, July 2003.
- [29] J. N. Fuchs, X. Leyronas, and R. Combescot. Hydrodynamic modes of a one-dimensional trapped Bose gas. *Phys. Rev. A*, 68(4):043610, October 2003.
- [30] the box  $L$  is chosen to be about twice the size of the cloud.
- [31] Note that we did not use Eq. (5) to compute  $\langle |\tilde{\rho}(q)|^2 \rangle_{\text{th}}$  since, for  $qR_{TF} \gtrsim 50$ ,  $\hbar q t_v / m \gtrsim 0.5$  and the approximation of Eq. (5) overestimates the density ripples by about 30%.
- [32] The transverse size of the cloud after the time-of-flight is comparable to the depth of focus of the imaging system and depends on the transverse confinement. We thus expect slightly different optical resolutions,  $\sigma_i$  and  $\sigma_f$  for data taken before and after the quench respectively. We correct for this effect to make quantitative comparison of data taken before and after the quench.
- [33] At a time  $t = t_{\text{th}}^q$  the  $g_1$  function has reached the ther-

- mal value  $e^{-|z|/l_c^f}$  for all  $z < 2l_c^f$ , the deviation from this thermal state being restricted to long distances where  $g_1(z) < e^{-2} \approx 10\%$ .
- [34] A. Johnson, S. S. Szigeti, M. Schemmer, and I. Bouchoule. Long-lived nonthermal states realized by atom losses in one-dimensional quasicondensates. *Phys. Rev. A*, 96(1):013623, July 2017.
- [35] Aditi Mitra. Quantum quench dynamics. *arXiv:1703.09740 [cond-mat]*, March 2017. arXiv: 1703.09740.
-

## Supplemental Materials: Cooling by three-body losses

This Supplementary Material gives technical information and details of calculations related to our paper entitled “Monitoring squeezed collective modes of a 1D Bose gas after an interaction quench using density ripples analysis”, referred to as the “main text”. In the first section we give a general derivation of the density ripples power spectrum, which does not *a priori* assume a homogeneous system. The second section gives the result for a homogeneous system and the analytical prediction for thermal equilibrium[S1]. The third section details the derivation of the density ripple power spectrum for a trapped gas, computed using the results for homogeneous gases and the local density approximation. The fourth section provides the explicit calculation of the post-quench evolution of the power spectrum for a harmonically trapped gas, namely the calculation of the function  $\mathcal{F}$  of the main text. In the fifth section, we verify the validity of the local density approximation for the parameters of the data presented in the main text. For this purpose, we compute the density ripple power spectrum using the Bogoliubov modes of the trapped gas. In the sixth section, we justify that interactions play a negligible role during time-of-flight, so that the calculations of the density ripples power spectrum, which assume instantaneous switch-off of the interactions, are valid. In the seventh section, we investigate two effects that are responsible for a reduction of the oscillation amplitude of the quantity  $\bar{J}(\tau)$ , extracted from the data, as compared to the simple theoretical predictions Eq. (6) of the main text: First the finite ramp time of the interaction strength decreases the squeezing of the collective modes, and second the finite resolution in  $\tau$  resulting from data binning is responsible for a decrease of the expected oscillation amplitude on the processed data.

### DERIVATION OF THE DENSITY RIPPLES POWER SPECTRUM

The power spectrum of density ripples has been first investigated in the limit of small density ripples and for a gas initially in the 3D Thomas-Fermi regime (*i.e.*  $\mu \gg \hbar\omega_\perp$ ) [S2, S3]. It was then computed assuming instantaneous switching off of the interactions in [S4]. Here, for consistency, we rederive Eq. (4) and (5) of the main text. Since we will later consider trapped gases, let us first assume a general scenario where we do not restrict ourselves to the homogeneous case. We let the gas evolve freely for a time  $t_f$  after interactions have been switched off. The power spectrum of the density fluctuations after  $t_f$  writes

$$\langle |\tilde{\rho}(q)|^2 \rangle = \int \int dz_1 dz_2 e^{iq(z_1 - z_2)} \langle \delta n(z_1, t_f) \delta n(z_2, t_f) \rangle. \quad (\text{S1})$$

Writing  $\delta n(z) = n(z) - \langle n(z) \rangle$  and expanding the above equation, the term  $|\int dz e^{iqz} \langle n(z, t_f) \rangle|^2$  appears. Here we consider times of flight short enough so that the shape of the cloud barely changes during time of flight, so that  $\langle n(z, t_f) \rangle \simeq \langle n(z, 0) \rangle$ . We moreover consider wavevectors  $q$  much larger than the inverse of the cloud length, such that  $|\int dz e^{iqz} \langle n(z, 0) \rangle|^2$  is a negligible quantity. We then have

$$\langle |\tilde{\rho}(q)|^2 \rangle \simeq \int \int dz_1 dz_2 e^{iq(z_1 - z_2)} \langle n(z_1, t_f) n(z_2, t_f) \rangle. \quad (\text{S2})$$

To compute  $n(z, t_f) = \Psi^\dagger(z, t_f) \Psi(z, t_f)$  we evolve the atomic field with the free-particle propagator, which leads to

$$\psi(z, t_f) = \frac{1}{\sqrt{2\pi t_f}} \int d\alpha \psi(\alpha, 0) e^{i\frac{(z-\alpha)^2}{2t_f}}, \quad (\text{S3})$$

where for simplicity we use a unit system in which  $m = \hbar = 1$ . We then have

$$\langle n(z_1, t_f) n(z_2, t_f) \rangle = \frac{1}{(2\pi t_f)^2} \int \int \int \int d\alpha d\beta d\gamma d\delta \langle \psi_\alpha^\dagger \psi_\beta \psi_\gamma^\dagger \psi_\delta \rangle e^{-i\frac{(z_1-\alpha)^2}{2t_f}} e^{i\frac{(z_1-\beta)^2}{2t_f}} e^{-i\frac{(z_2-\gamma)^2}{2t_f}} e^{i\frac{(z_2-\delta)^2}{2t_f}}, \quad (\text{S4})$$

where we use the simplified notation  $\psi_\nu = \psi(\nu, 0)$ . Expanding the exponentials, the above expression writes

$$\langle n(z_1, t_f) n(z_2, t_f) \rangle = \frac{1}{(2\pi t_f)^2} \int \int \int \int d\alpha d\beta d\gamma d\delta \langle \psi_\alpha^\dagger \psi_\beta \psi_\gamma^\dagger \psi_\delta \rangle e^{i\frac{(\alpha-\beta)z_1}{t_f}} e^{i\frac{\beta^2 - \alpha^2}{2t_f}} e^{i\frac{(\gamma-\delta)z_2}{t_f}} e^{i\frac{\delta^2 - \gamma^2}{2t_f}}. \quad (\text{S5})$$

Injecting into Eq. (S2), and using  $\int dz e^{ikz} = 2\pi\delta(k)$  and  $\delta(x/\alpha) = \alpha\delta(x)$ , we get

$$\langle |\tilde{\rho}(q)|^2 \rangle = \int \int d\alpha d\delta \langle \psi_\alpha^\dagger \psi_{\alpha+qt_f} \psi_{\delta+qt_f}^\dagger \psi_\delta \rangle e^{-i\frac{\alpha^2}{2t_f}} e^{i\frac{(\alpha+qt)^2}{2t_f}} e^{-i\frac{(\delta+qt)^2}{2t_f}} e^{i\frac{\delta^2}{2t_f}}. \quad (\text{S6})$$



Defining  $\delta = \alpha + X$ , we obtain

$$\langle |\tilde{\rho}(q)|^2 \rangle = \int \int d\alpha dX e^{iqX} \langle \psi_\alpha^+ \psi_{\alpha+qt_f} \psi_{\alpha+X+qt_f}^+ \psi_{\alpha+X} \rangle. \quad (\text{S7})$$

For gases lying deep in the quasi-condensate regime, one can neglect density fluctuations when estimating the expectation value in the above equation, such that

$$\langle |\tilde{\rho}(q)|^2 \rangle \simeq \int \int d\alpha dX e^{iqX} \sqrt{n(\alpha)n(\alpha+qt_f)n(\alpha+X+qt_f)n(\alpha+X)} \langle e^{i(\theta(\alpha)-\theta(\alpha+qt_f)+\theta(\alpha+X+qt_f)-\theta(\alpha+X))} \rangle. \quad (\text{S8})$$

The following section applies this result to homogeneous systems. This equation is however not restricted to homogeneous systems and we will use it to treat the effect of the trap beyond the local density approximation.

## POWER SPECTRUM OF THE DENSITY RIPPLES FOR A HOMOGENEOUS GAS

For a homogeneous gas, the relevant quantity is an intensive variable which relates to the expression  $\langle |\tilde{\rho}(q)|^2 \rangle$  of the previous section by

$$\langle |\rho(q)|^2 \rangle = \frac{1}{L} \langle |\tilde{\rho}(q)|^2 \rangle \quad (\text{S9})$$

where  $L$  is the length of the box. Injecting Eq. (S8) into Eq. (S9), we recover Eq. (3) and (4) of the main text, up to an irrelevant term in  $\delta(q)$  [S5]. In fact, Wick's theorem is applicable since  $\theta$  is a Gaussian variable [S6], which leads to

$$\langle |\rho(q)|^2 \rangle = n_0^2 \int dX e^{iqX} e^{-\frac{1}{2} \langle (\theta(0) - \theta(qt_f) + \theta(X+qt_f) - \theta(X))^2 \rangle}. \quad (\text{S10})$$

To compute the power spectrum of density ripples for a thermal equilibrium state, we follow the calculation made in [S4] and expand the exponential term in Eq. (S10) as a function of the first order correlation function  $g^{(1)}(z) = n_0 e^{-\frac{1}{2} \langle (\theta(0) - \theta(z))^2 \rangle}$ , which fulfils  $g^{(1)}(z) = n_0 e^{-|z|/l_c}$  where  $l_c = 2\hbar^2 n_0 / (k_B T)$  [S4]. Calculation of the integral in Eq. (S10) then leads to

$$\langle |\rho(q)|^2 \rangle = 2n_0^2 \frac{2ql_c - 2e^{-2\hbar q t_f / (ml_c)} (ql_c \cos(\hbar q^2 t_f / m) + 2 \sin(\hbar q^2 t_f / m))}{q(4 + l_c^2 q^2)}. \quad (\text{S11})$$

Note that we corrected the formula given in [S4]. The power spectrum computed with this equation is compared in Fig. S1 to the approximated formula valid for small  $q$ , namely Eq. (5) of the main text.

## DENSITY RIPPLE SPECTRUM FOR A HARMONICALLY CONFINED GAS UNDER THE LOCAL DENSITY APPROXIMATION (LDA)

Let us investigate the density ripples power spectrum in the case of a gas trapped in a longitudinal potential smooth enough so that the cloud size  $L$  is much larger than the typical phase correlation length  $l_c$  and much larger than  $\hbar q t_f / m$ :  $L \gg l_c, \hbar q t_f / m$ . As in section , we moreover consider the power spectrum for wavevectors  $q \gg 1/L$ . Let us start with the general expression Eq. (S1) that we write

$$\langle |\tilde{\rho}(q)|^2 \rangle = \int dz \int du \langle \delta\rho(z, t_f) \delta\rho(z + u, t_f) \rangle e^{iqu}. \quad (\text{S12})$$

Consider  $\langle \delta\rho(z, t_f) \delta\rho(z + u, t_f) \rangle$  for a given  $z$ . This expression vanishes over a length much smaller than  $L$ , so values of  $u$  significantly contributing to the integral are much smaller than  $L$ . Moreover the region of the initial cloud contributing most to  $\langle \delta\rho(z, t_f) \delta\rho(z + u, t_f) \rangle$  is much smaller than  $L$  for sufficiently large  $L$ . Then, to compute  $\langle \delta\rho(z, t_f) \delta\rho(z + u, t_f) \rangle$  one can perform a local density approximation and use the result of a homogeneous gas at a density  $n_0(z)$ . We then obtain

$$\langle |\tilde{\rho}(q)|^2 \rangle = \int dz \langle |\rho_{n_0(z)}(q)|^2 \rangle \quad (\text{S13})$$

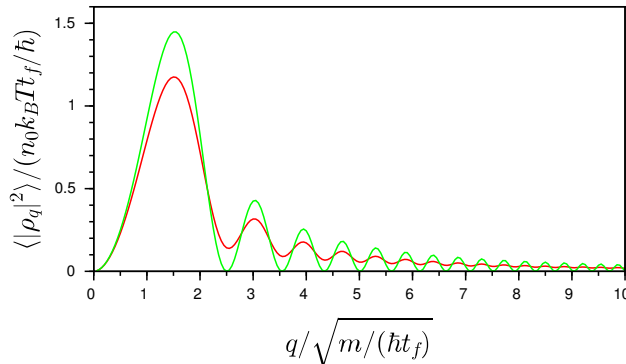


FIG. S1. Density ripples power spectrum for a homogeneous gas. The exact formula Eq. (S11) (red curve) is compared to the small  $q$  approximation given Eq. (5) of the main text, where  $\langle |\rho(q)|^2 \rangle$  is proportional to  $\langle \theta_q^2 \rangle$  (green curve). The only relevant parameter is  $\hbar t_f / (m l_c^2)$ . Results are shown for  $\hbar t_f / (m l_c^2) = 0.05$ , a value corresponding to the data depicted in Fig. (2,b) of the main text, the correlation length  $l_c = 2\hbar^2 n_0 / (m k_B T)$  being computed for the central density. The effect of the imaging resolution is to multiply this theoretical power spectrum with  $e^{-\sigma^2 q^2}$ , where  $\sigma$  is the rms width of the imaging pulse response function, assumed to be Gaussian. For our data,  $\sigma \sqrt{m / (\hbar t_f)} = 0.85$  and only the first maximum of  $\langle |\rho(q)|^2 \rangle$  remains visible.

where the subscript  $n_0(z)$  specifies that one considers the result for a homogeneous gas of density  $n_0(z)$ . This expression is referred to as the local density approximation expression (LDA) of the power spectrum. We have tested this approximation, for conditions close to the experimental data presented in the main text, by comparing it with calculations based on the Bogoliubov excitations of the trapped system (see section ).

### EVOLUTION OF THE DENSITY RIPPLE POWER SPECTRUM FOR A HARMONICALLY CONFINED GAS UNDER THE LDA

Here we give an explicit derivation of Eq. (6) of the main text, for a gas harmonically confined in a longitudinal trap of frequency  $\omega_{\parallel}$ . Injecting Eq. (5) and Eq. (2) of the main text into Eq. (S13), and using the local initial power spectrum of  $\theta$  which writes  $\langle \theta_q^2 \rangle = m k_B T / (\hbar^2 n_0 q^2)$ , we derive Eq. (6) of the main text with

$$\mathcal{F} = \int dz n_0(z) \sin^2(c(z)qt) / N \quad (\text{S14})$$

where  $N$  is the total atom number. The density profile  $n_0(z)$  is estimated itself within the LDA, using the local chemical potential

$$\mu(z) = \mu_p (1 - (z/R_{\text{TF}})^2), \quad (\text{S15})$$

where  $R_{\text{TF}}$  is the Thomas-Fermi radius of the density profile and  $\mu_p$  is the chemical potential at the trap center. For a transverse harmonic confinement of frequency  $\omega_{\perp}$ , it has been checked, by comparing with predictions of the 3D Gross-Pitaevskii equation, that the equation of state of the gas is very well described by the heuristic formula [S7]

$$\mu(n) = \hbar \omega_{\perp} (\sqrt{1 + 4na} - 1), \quad (\text{S16})$$

where  $a$  is the 3D scattering length between atoms. For small linear densities, we recover the 1D expression  $\mu = 2\hbar \omega_{\perp} a n$ , valid far from the confinement-induced resonance [S8]. Using Eq. (S16) and Eq. (S15), we obtain the density profile

$$n_0(z) = \left[ (\eta(1 - \tilde{z}^2) + 1)^2 - 1 \right] / (4a) \quad (\text{S17})$$

where we introduced  $\tilde{z} = z/R_{\text{TF}}$  and  $\eta = \mu_p / (\hbar \omega_{\perp})$ . This yields  $N = (4/3\eta + 8\eta^2/15) R_{\text{TF}} / (2a)$ . The local speed of sound on the other hand, obtained from the thermodynamic relation  $c = \sqrt{n(\partial\mu/\partial n)/m}$ , writes

$$c(z) = c_p \sqrt{\frac{(1 + \eta) \left[ (1 + \eta(1 - \tilde{z}^2))^2 - 1 \right]}{(1 + \eta(1 - \tilde{z}^2)) ((1 + \eta)^2 - 1)}}, \quad (\text{S18})$$

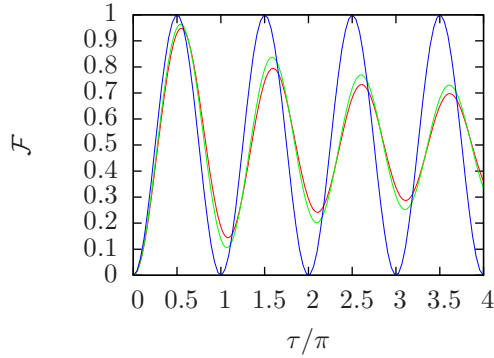


FIG. S2. Oscillation of each spectral component of the power spectrum for a harmonically confined gas in the LDA. The function  $\mathcal{F}$  is shown in green, for  $\eta = \mu_p/(\hbar\omega_\perp) = 1.0$ . The pure 1D limit, corresponding to  $\eta \ll 1$  is shown in red. The oscillations expected for a homogeneous gas are shown in blue. In all the cases,  $\tau = cqt$  where  $c$  is the central sound velocity.

where  $c_p$  is the speed of sound computed for the central density. Injecting into Eq. (S14), we then find

$$\mathcal{F} = \frac{1}{4\eta/3 + 8\eta^2/15} \int_0^1 d\tilde{z} \left[ (1 + \eta(1 - \tilde{z}^2))^2 - 1 \right] \sin^2 \left( \tau \sqrt{\frac{(1 + \eta) \left[ (1 + \eta(1 - \tilde{z}^2))^2 - 1 \right]}{(1 + \eta(1 - \tilde{z}^2)) ((1 + \eta)^2 - 1)}} \right). \quad (\text{S19})$$

When the gas is deeply 1D, namely for  $\eta \ll 1$ , this expression reduces to

$$\mathcal{F}_{\text{1D}} = \frac{3}{2} \int_0^1 d\tilde{z} (1 - \tilde{z}^2) \sin^2 \left( \tau \sqrt{1 - \tilde{z}^2} \right). \quad (\text{S20})$$

Experimentally, values of  $\eta$  are in the range  $[0.6; 1.3]$ . Fig. S2 shows the function  $\mathcal{F}$ , computed for  $\eta = 1$ . We compare it to  $\mathcal{F}_{\text{1D}}$  and to the expression expected for a homogeneous gas, namely  $\sin^2(\tau)$ .

### BEYOND THE LOCAL DENSITY APPROXIMATION: CALCULATION USING BOGOLIUBOV MODES OF A HARMONICALLY CONFINED 1D GAS

Here we consider a 1D gas confined longitudinally in a harmonic trap of frequency  $\omega_\parallel$ . In opposition to the calculations done in the previous section we do not rely on the local density approximation but use the Bogoliubov modes of the trapped gas to compute the post-quench evolution and the density ripples power spectrum. The relevant collective modes lie deep in the phononic regime. The Bogoliubov modes, indexed by an integer  $\nu$ , then acquire an analytical dispersion relation and analytical wavefunctions that one can use for calculations. For each mode, the dynamics are accounted for by the harmonic oscillator Hamiltonian

$$H_\nu = \hbar\omega_\nu \left( \frac{x_\nu^2}{2} + \frac{p_\nu^2}{2} \right), \quad (\text{S21})$$

where  $\omega_\nu = \omega_\parallel \sqrt{\nu(\nu+1)/2}$  and  $x_\nu$  and  $p_\nu$  are canonically conjugate variables. The phase and density fluctuation operators write

$$\begin{cases} \theta(z) = \sum_\nu \theta_\nu(z) p_\nu \\ \delta n(z) = \sum_\nu n_\nu(z) x_\nu \end{cases} \quad (\text{S22})$$

where

$$\begin{cases} \theta_\nu(z) = \frac{1}{\sqrt{2}} \left( \frac{mg}{\hbar^2 n_p} \right)^{1/4} \frac{\sqrt{2\nu+1}}{(\nu(\nu+1))^{1/4}} P_\nu(z/R_{TF}) \\ n_\nu(z) = \frac{\sqrt{2\nu+1}}{2R_{TF}} (\nu(\nu+1))^{1/4} \left( \frac{\hbar^2 n_p}{mg} \right)^{1/4} P_\nu(z/R_{TF}). \end{cases} \quad (\text{S23})$$

Here  $n_p$  and  $R_{TF}$  are the central density and radius of the Thomas-Fermi profile  $n_0(z) = n_p(1 - (z/R_{TF})^2)$ . The interaction quench consists of a sudden change of the interaction parameter  $g$  from  $g_i$  to  $g_f = (1 + \kappa)g_i$  at  $t = 0$ , while changing the longitudinal oscillation frequency by a factor  $\sqrt{1 + \kappa}$  so that  $R_{TF}$  stays constant. Then the interaction quench preserves the shapes of the wavefunctions  $\theta_\nu$  and  $n_\nu$ , and it simply changes the canonical variables  $x_\nu$  and  $p_\nu$  according to

$$\begin{cases} x_\nu(t = 0^+) = (g_f/g_i)^{1/4}x_\nu(t = 0^-) \\ p_\nu(t = 0^+) = (g_i/g_f)^{1/4}p_\nu(t = 0^-) \end{cases} \quad (\text{S24})$$

Under such a transformation, the initial thermal state, an isotropic Gaussian, becomes a squeezed state and its subsequent evolution under the Hamiltonian Eq. (S21) leads to a breathing of each quadrature. In particular

$$\langle p_\nu^2 \rangle = \langle p_\nu^2 \rangle_i (1 + \kappa \sin^2(\omega_\nu t)). \quad (\text{S25})$$

The initial value  $\langle p_\nu^2 \rangle_i$  is given by the thermal expectation value, which reduces to

$$\langle p_\nu^2 \rangle_i = k_B T / (\hbar \omega_\nu) \quad (\text{S26})$$

for the low-lying modes for which  $k_B T \gg \hbar \omega_\nu$ .

Injecting Eq. (S22) into Eq. (S8), using Wick's theorem and the fact that different modes are uncorrelated we get

$$\langle |\tilde{\rho}(q)|^2 \rangle = \int \int d\alpha dX e^{iqX} \sqrt{n_0(\alpha)n_0(\alpha + qt_f)n_0(\alpha + X + qt_f)n_0(\alpha + X)} e^{-\frac{1}{2} \sum_\nu \langle p_\nu^2 \rangle (\theta_\nu(\alpha) - \theta_\nu(\alpha + qt_f) + \theta_\nu(\alpha + X + qt_f) - \theta_\nu(\alpha + X))^2}. \quad (\text{S27})$$

For  $\hbar qt_f/m \ll l_c$ , where  $l_c$  is the phase correlation length, one can expand the exponential and  $\langle |\tilde{\rho}(q)|^2 \rangle$  is obtained by summing the contribution of each mode. Since the Legendre polynomials behave as  $\cos((\nu + 1/2)x + \pi/4)$  at small  $x$ , the contribution of the mode  $\nu$  is peaked at  $q \simeq \nu/R_{TF}$ .

The predictions of Eq. (S27) may be compared to the one obtained within the Local density approximation. Here we focus on the case of thermal equilibrium. We compute the density ripple spectrum injecting the thermal equilibrium value Eq. (S26) and the mode wavefunction Eq. (S23) into Eq. (S27). Fig. S3 shows the result for a cloud whose Thomas-Fermi radius fulfils  $l_c/R_{TF} = 0.2$ , where  $l_c = 2\hbar^2 n_p / (mk_B T)$  is the correlation length of the first order correlation function at the center of the cloud, and for a time-of-flight  $t_f = 6 \times 10^{-4} m R_{TF}^2 / \hbar$ . These parameters are close to the experimental ones. We compared the results with the LDA, together with the analytical formula for homogeneous gases Eq. (S11) and we find excellent agreement. We also compare with the LDA but using, instead of Eq. (S11), the approximation Eq. 5 of the main text. We find very good agreement as long as  $qR_{TF} < 50$ .

## BEYOND INSTANTANEOUS INTERACTION SWITCH OFF : FINITE TRANSVERSE EXPANSION TIME

In the data presented in the main text, the frequency of the probed longitudinal modes, of the order of  $cq$ , is no more than  $0.15 \times \omega_\perp$ . Then, due to the rapid transverse expansion, interactions during time-of-flight become almost instantaneously negligible and are expected to give only minor corrections to the density ripples spectrum computed for an instantaneous switching off of the interactions. It is nevertheless interesting to estimate their effect. This has already been computed in [S3], in the limit  $\mu \gg \hbar \omega_\perp$  and using time-dependent Bogoliubov equations, *i.e.* equations of motion linearized in density fluctuations and phase gradient. The linearized calculations *a priori* require that density fluctuations stay small. Although in our case density ripples at the end of the time-of-flight have large amplitudes, the Bogoliubov calculations hold for the small  $q$  components, which fulfil  $ql_c \ll t_f$  and which are considered in our paper. The condition  $\mu \gg \hbar \omega_\perp$  on the other hand is not verified for the data shown in the main text. We nevertheless believe that the calculations of [S3] give a relevant estimation of the effect of interactions during the time-of-flight for our data. From results of [S3], we find that the density ripples power spectrum for the small  $q$  wavevectors, given by equation (5) of the main text, should be corrected by the factor

$$\mathcal{C} = (\omega_\perp t_f)^{-\left(\frac{ck}{\omega_\perp}\right)^2}. \quad (\text{S28})$$

In all experimental situations  $\mathcal{C} > 0.95$ , which confirm that the effect of interactions during the time-of-flight is small.

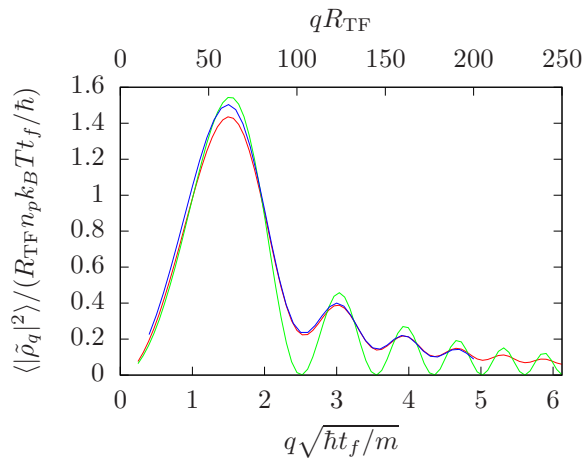


FIG. S3. Test of the local density approximation (LDA). The plot shows the density ripples spectrum of a gas at thermal equilibrium confined in a harmonic potential. The complete calculation, based on the expansion on the Bogoliubov modes, whose wavefunctions are given by the Legendre polynomial, is shown in blue. It is in excellent agreement with the spectrum computed within the local density approximation (LDA) shown in red. The further approximation of small wavevectors, Eq. (5) of the main text, injected into the LDA, shown in green, is also in good agreement, for wavevectors fulfilling  $qR_{\text{TF}} < 50$ . Calculations are done for a Thomas-Fermi radius  $l_c/R_{\text{TF}} = 0.2$  and time-of-flight  $t_f = 0.015ml_c^2/\hbar$ , where  $l_c = 2\hbar^2 n_p / (mk_B T)$  is the correlation length at the center of the cloud. These parameters are close to those of the experimental data.

### EFFECTS THAT MAY REDUCE THE DENSITY RIPPLES POWER SPECTRUM OSCILLATION AMPLITUDE

In this section we investigate two effects responsible for a reduction of the amplitude of the oscillations of  $\bar{J}$  (see main text), as compared to the theoretical prediction given by Eq. (6) of the main text. We first consider the effect of the finite ramp time of the interaction strength, which reduces the squeezing of the Bogoliubov modes, as compared to an instantaneous quench. This effect contributes to the reduction of the amplitude on the order of 10%. We then investigate the reduction of the amplitude induced by the binning of the data with a finite resolution in  $\tau$ . This effect amounts to an additional reduction of the amplitude by 18%.

#### Beyond the instantaneous quench : finite ramp time of the interaction strength

In the experiment, the change of the effective interaction strength is not instantaneous: to ensure the adiabatic following of the transverse motion, we perform a ramp of the transverse oscillation frequency during a time  $t_r$ . The finite value of  $t_r$  is responsible for a decrease of the induced squeezing of each mode. In the asymptotic limit of very large  $t_r$ , the squeezing vanishes since then, the modes follow adiabatically the modification of the interaction strength. In the following we compute the effect of the ramp on the squeezing of each mode and we use this result to compute the resulting decrease of the oscillation amplitude of  $\bar{J}$ .

In order to estimate the effect of the finite ramp time, we will consider a homogeneous gas for simplicity. The Bogoliubov modes are then described by the Hamiltonian of Eq. (1) of the main text, namely

$$H_q = A_q n_q^2 + B_q \theta_q^2. \quad (\text{S29})$$

We regard the effect of a ramp of  $\omega_\perp$  between the time  $t = 0$  and the time  $t_r$ :  $\omega_\perp$  goes from  $\omega_\perp^i$  to  $\omega_\perp^f = (\kappa + 1)\omega_\perp^i$ , as depicted in Fig. (S4). The coefficient  $B_q = n_0 \hbar^2 q^2 / (2m)$  is time-independent, while the coefficient  $A_q$  evolves linearly during the ramp (*i.e.* during time interval  $0 < t < t_r$ ), since it is proportional to  $c^2$ , itself proportional to  $\omega_\perp$ . Then, the solution of the second order equations describing the evolution of  $\theta_q$  and  $n_q$  during the ramp is given in terms of the Airy functions. In order to investigate the squeezing, it is natural to introduce the reduced variables

$$\begin{cases} \tilde{\theta}_q = \theta_q / \bar{\theta}_q \\ \tilde{n}_q = n_q / \bar{n}_q \end{cases} \quad (\text{S30})$$

where  $\tilde{\theta}_q = (A_q(t)/B_q)^{1/4}$  and  $\tilde{n}_q = (B_q/A_q(t))^{-1/4}$  are the time-dependent widths of the ground state. For given initial values, the values of  $\tilde{\theta}_q$  and  $\tilde{n}_q$  at the end of the ramp are

$$\begin{pmatrix} \tilde{\theta}_q(t_r) \\ \tilde{n}_q(t_r) \end{pmatrix} = M \begin{pmatrix} \tilde{\theta}_q(0) \\ \tilde{n}_q(0) \end{pmatrix} \quad (\text{S31})$$

where the matrix  $M$  has the following components:

$$\begin{cases} M_{11} = (\kappa + 1)^{-1/4} \pi (-B_i(-\delta^{-2/3})A'_i(-(\kappa + 1)\delta^{-2/3}) + A_i(-\delta^{-2/3})B'_i(-(\kappa + 1)\delta^{-2/3})) \\ M_{22} = (\kappa + 1)^{1/4} \pi (B'_i(-\delta^{-2/3})A_i(-(\kappa + 1)\delta^{-2/3}) - A'_i(-\delta^{-2/3})B_i(-\delta^{-2/3}(\kappa + 1))) \\ M_{21} = (\delta^{-4/3}(\kappa + 1))^{1/4} \pi (-B_i(-\delta^{-2/3})A_i(-\delta^{-2/3}(\kappa + 1)) + A_i(-\delta^{-2/3})B_i(-\delta^{-2/3}(\kappa + 1))) \\ M_{12} = (\delta^{-4/3}(\kappa + 1))^{-1/4} \pi (B'_i(-\delta^{-2/3})A'_i(-\delta^{-2/3}(\kappa + 1)) - A'_i(-\delta^{-2/3})B'_i(-\delta^{-2/3}(\kappa + 1))) \end{cases} \quad (\text{S32})$$

Here  $A_i, B_i$  are the first and second kind Airy functions and  $A'_i, B'_i$ , their derivatives and  $\delta = \kappa/(t_r \omega_q^i)$  the quench speed normalized to the initial mode frequency (we recall that the quench strength is  $\kappa = \omega_\perp^f/\omega_\perp^i - 1$ ). Under this transformation, the initial isotropic Gaussian distribution transforms into a squeezed distribution, *i.e.* a Gaussian elliptical distribution with a squeezing angle  $\alpha$  and ratio between the rms width of the two eigenaxes equal to the squeezing factor  $S$ . In order to find  $\alpha$  and  $S$ , let us compute, for any angle  $\beta$ , the width along the quadrature  $\tilde{x}_\beta = \cos(\beta)\tilde{\theta}_q + \sin(\beta)\tilde{n}_q$ . Using the fact that the initial state is a thermal equilibrium state fulfilling  $\langle \tilde{\theta}_q^2 \rangle_i = \langle \tilde{n}_q^2 \rangle_i \equiv V$  and  $\langle \tilde{\theta}_q \tilde{n}_q \rangle_i = 0$ , and using the transformation above, we find

$$\langle \tilde{x}_\beta^2 \rangle = V (\cos^2(\beta) (M_{11}^2 + M_{22}^2) + \sin^2(\beta) (M_{21}^2 + M_{12}^2) + 2 \cos(\alpha) \sin(\alpha) (M_{11}M_{21} + M_{22}M_{12})). \quad (\text{S33})$$

The squeezing angle  $\alpha$  is found by imposing  $d\langle \tilde{x}_\beta^2 \rangle/d\beta|_{\beta=\alpha} = 0$ , which leads to

$$\tan(2\alpha) = -2 \frac{M_{11}M_{21} + M_{22}M_{12}}{M_{21}^2 + M_{22}^2 - M_{11}^2 - M_{12}^2}. \quad (\text{S34})$$

The most squeezed quadrature is  $\tilde{x}_\alpha$  while  $\tilde{x}_{\alpha+\pi/2}$  is the most anti-squeezed quadrature. The squeezing factor is  $S = \sqrt{\langle \tilde{x}_\alpha^2 \rangle} / \sqrt{\langle \tilde{x}_{\alpha+\pi/2}^2 \rangle}$ . It also writes  $S = \langle \tilde{x}_\alpha^2 \rangle / V$  since the conservation of the phase-space area ensures  $\sqrt{\langle \tilde{x}_\alpha^2 \rangle \langle \tilde{x}_{\alpha+\pi/2}^2 \rangle} = V$ , and it is evaluated injecting  $\beta = \alpha$  in Eq. (S33). Results are shown in Fig. (S4) for quench amplitudes  $\kappa = 2$  and  $\kappa = 4$  as a function of  $\omega_q^f t_r$  where  $\omega_q^f$  is the final frequency of the mode. For very slow modes  $\omega_q^f t_r \ll 1$ , one recovers the results expected for an instantaneous quench :  $\alpha \simeq 0$  and  $(S^2 - 1) \simeq \kappa$ . For modes of larger frequency, the effect of the ramp is to reduce the squeezing and also to rotate its axis.

The post-quench dynamics results in a breathing of the  $\tilde{\theta}_q$  quadrature:  $\langle \tilde{\theta}_q^2 \rangle$  oscillates with an amplitude  $V(S^2 - 1)/S$ . Coming back to the variable of  $\theta_q$ , the evolution at times  $t > t_r$  writes

$$\langle \theta_q^2 \rangle(t) = \langle \theta_q^2 \rangle_i \frac{\sqrt{\kappa + 1}}{S_q} (1 + (S_q^2 - 1) \sin^2(\omega_q^f(t - t_r) + \alpha_q)) \quad (\text{S35})$$

where the indice  $q$  in  $S$  and  $\alpha$  indicates these quantities depend on  $q$ . As seen in Fig. (S4), the angle  $\alpha_q$  is very close to  $\omega_q^f t_r / 2$ , for moderate values of  $\omega_q^f t_r$ . Injecting this value into Eq. (S35), we find that it amounts to shifting the time reference to  $t_r/2$ . We perform this shift when analyzing the data, in other terms the reduced variable  $\tau$  is  $\tau = cq(t - t_r/2)$ .

Let us now consider the evolution of the density-ripples power spectrum  $\langle |\tilde{\rho}_q|^2 \rangle(t)$ . For small  $q$ ,  $\langle |\tilde{\rho}_q|^2 \rangle(t)$  is proportional to  $\langle \theta_q^2 \rangle(t)$  such that the evolution of  $\langle |\tilde{\rho}_q|^2 \rangle(t)$  is given by Eq. (S35). This leads to,

$$J(q, \tau) = \frac{\langle |\tilde{\rho}_q|^2 \rangle(t = \tau/(cq))}{\langle |\tilde{\rho}_q|^2 \rangle_i} = \frac{\sqrt{\kappa + 1}}{S_q} (1 + (S_q^2 - 1) \sin^2(\tau)). \quad (\text{S36})$$

Let us now investigate the quantity  $\bar{J}(\tau)$ , defined in the main text for experimental data. Here we will assume that the measurement times are spread over  $[t_m, t_M]$  and we denote  $h(t)dt$  the number of points in the time interval  $[t, t + dt]$ . The  $q$  values are assumed to be equally spaced, as in the case of a Fast Fourier Transform, and only  $q$  values in the interval  $[q_m, q_M]$  are considered. We assume that  $\bar{J}(\tau)$  is obtained by binning in  $\tau$  the collection of data with a bin size  $\Delta$  small enough so that, for all measurement times  $t$ ,  $J(q, \tau)$  is about constant in the interval  $q \in [\tau/(ct), (\tau + \Delta)/(ct)]$ . Then, one has

$$\bar{J}(\tau) = \frac{1}{\int h(t)dt \Delta/(ct)} \int h(t)dt J(q = \tau/(ct), \tau) \Delta/(ct), \quad (\text{S37})$$

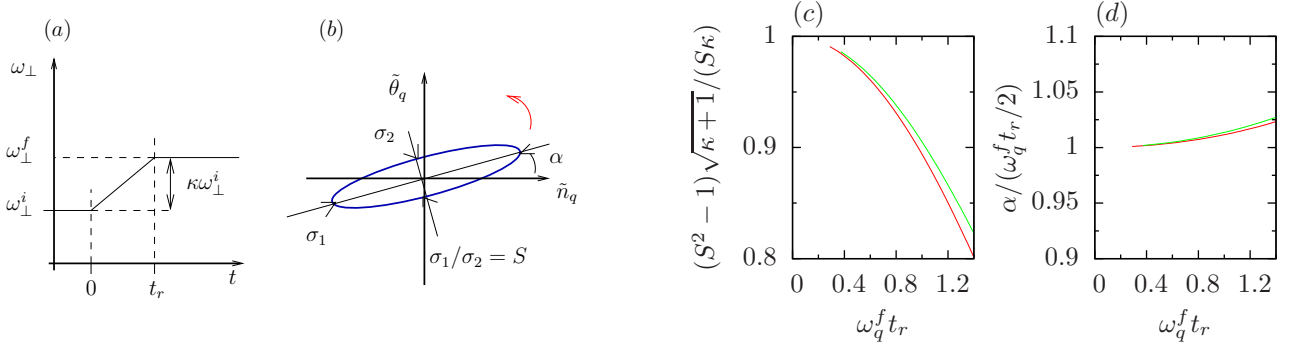


FIG. S4. Effect of the interaction strength ramp on the squeezing of longitudinal modes. The time sequence is shown in (a). An example of the phase space distribution at the end of the ramp is shown in (b): the  $1/\sqrt{e}$  line of the Gaussian distribution is plotted. The squeezing factor  $S$  is the ratio between the rms widths along the anti-squeezed and the squeezed directions. The red arrow shows the direction of rotation under free evolution. Quantitative results are shown in (c) and (d) for a quench strength  $\kappa = \omega_{\perp}^f/\omega_{\perp}^i - 1 = 2$  (red lines) and  $\kappa = 4$  (green lines). (c) shows  $\sqrt{\kappa+1}(S^2-1)/(S\kappa)$ , which gives the amplitude of the resulting breathing oscillations normalized to the amplitude for an instantaneous quench (see text), versus  $\omega_q^f t_r$  where  $\omega_q^f$  is the final frequency of the mode. The squeezing angle is shown in (d), normalized by  $\omega_q^f t_r/2$ .

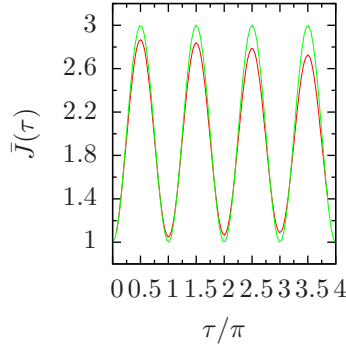


FIG. S5. Effect of the finite ramp time of the interaction strength for a homogeneous gas. The expected behavior of  $\bar{J}$  (red) is compared to the case of an instantaneous ramp (green). Here we consider a gas of Rubidium atoms at conditions close to the experimental ones. More precisely, the linear density is  $n_0 = 630$  atoms per  $\mu\text{m}$ , the initial transverse oscillation frequency is  $\omega_{\perp} = 2\pi \times 1.5$  kHz, the quench strength is  $\kappa = 2$  and the ramp time is  $t_r = 0.7$  ms. The range of  $q$  values used to compute  $\bar{J}$  is  $q \in [0.1, 0.5]\mu\text{m}^{-1}$  and the range of measurement times is  $t \in [t_r/2, 6\text{ms}]$ .

where the integrals are evaluated between  $t_1$  and  $t_2$ , where  $t_1 = \text{Max}(t_m, \tau/(c q_m))$  and  $t_2 = \text{Min}(t_m, \tau/(c q_m))$ . Typically, in the experiment small times are sampled more densely than large times. Taking  $h$  proportional to  $1/t$ , we obtain

$$\bar{J}(\tau) = \frac{1}{\int dt/t^2} \int dt J(q = \tau/(ct), \tau)/t^2 = \frac{\int dq J(q, \tau)}{q_2(\tau) - q_1(\tau)}, \quad (\text{S38})$$

where  $q_1 = \max(\tau/(c)t_m, q_m)$  and  $q_2 = \min(\tau/(c)t_m, q_m)$ .

The predicted time evolution of  $\bar{J}$  is shown in Fig. (S4) for parameters close to that of the experimental data shown in the main text. The amplitude of the first oscillation is decreased by about 10%.

### Finite width of the convolution function used in data processing

The data shown in the inset of Fig. (2) of the main text correspond to a data set with an exceptionally good signal over noise. In general, the spread of the data points corresponding to a given value of  $\tau$  (and thus corresponding to different times  $t$  and wavevectors  $q$ ) is as large as about 50%. In such conditions, a binning of the data as a function of the reduced time  $\tau = cqt$  with a bin size sufficiently large to accommodate many data points is required in order to increase the signal over noise. As describe in the main text, we use a “smooth” binning: we compute the weighted average of the data,  $\bar{J}$ , with a Gaussian cost function of rms width  $\Delta$ . For a very dense data set, we can define the local average value  $\tilde{J}(\tau) = \sum_{i, \tau_i \in [\tau, \tau+d\tau]} J_i/d\tau$ , where the sum is done on the data set and  $d\tau$  is much smaller than  $\Delta$ . Then  $\bar{J}$  corresponds to the convolution of  $\tilde{J}$  with a convolution width  $\Delta$ . This convolution reduces the amplitude of the oscillations. To estimate this amplitude reduction, let us disregard the small damping of the oscillations coming from the cloud inhomogeneity (see section 2) and thus consider data which would follow the oscillatory behavior  $\tilde{J} = A \sin^2(\tau)$ . The smoothing  $\bar{J}(\tau) = \int_{-\infty}^{\infty} d\tau' \tilde{J}(\tau') e^{-(\tau'-\tau)^2/(2\Delta^2)} / (\sqrt{2\pi}\Delta^2)$  reduces the amplitude to  $A' = Ae^{-2\Delta^2}$ . For  $\Delta = 0.1\pi$ , as used for the data analysis shown in the main text, the amplitude is reduced by 18%.

---

\* current adressVienna Center for Quantum Science and Technology, TU Wien-Atominstytut, Stadionallee 2, 1020 Vienna, Austria.

† isabelle.bouchoule@institutoptique.fr

[S1] We corrected the formula published in [S4].

[S2] S. Dettmer, D. Hellweg, P. Ryytty, J. J. Arlt, W. Ertmer, K. Sengstock, D. S. Petrov, G. V. Shlyapnikov, H. Kreutzmann, L. Santos, and M. Lewenstein. Observation of Phase Fluctuations in Elongated Bose-Einstein Condensates. *Phys. Rev. Lett.*, 87(16):160406, October 2001.

[S3] D. Hellweg, S. Dettmer, P. Ryytty, J. J. Arlt, W. Ertmer, K. Sengstock, D. S. Petrov, G. V. Shlyapnikov, H. Kreutzmann, L. Santos, and M. Lewenstein. Phase fluctuations in BoseEinstein condensates. *Appl Phys B*, 73(8):781–789, December 2001.

[S4] A. Imambekov, I. E. Mazets, D. S. Petrov, V. Gritsev, S. Manz, S. Hofferberth, T. Schumm, E. Demler, and J. Schmiedmayer. Density ripples in expanding low-dimensional gases as a probe of correlations. *Phys. Rev. A*, 80(3):033604, September 2009.

[S5] This term is due to the approximation made when going from Eq. (S1) to Eq. (S2), which is valid only for  $q$  values larger than the inverse of the cloud size.

[S6] Since the Hamiltonian of interest is quadratic in  $\theta$ , the distribution of  $\theta$  is Gaussian at thermal equilibrium. The squeezing of each collective mode produced by the interaction quench preserves the Gaussian nature of  $\theta$ .

[S7] J. N. Fuchs, X. Leyronas, and R. Combescot. Hydrodynamic modes of a one-dimensional trapped Bose gas. *Phys. Rev. A*, 68(4):043610, October 2003.

[S8] M. Olshanii. Atomic Scattering in the Presence of an External Confinement and a Gas of Impenetrable Bosons. *Phys. Rev. Lett.*, 81(5):938–941, August 1998.

---

\* current adressVienna Center for Quantum Science and Technology, TU Wien-Atominstytut, Stadionallee 2, 1020 Vienna, Austria.

† isabelle.bouchoule@institutoptique.fr